Long-term NR2B expression in the cerebellum alters granule cell development and leads to NR2A down-regulation and motor deficits

Schlett, K; Pieri, [No Value]; Metzger, F; Marchetti, L; Dere, E; Kirilly, D; Tarnok, K; Barabas, B; Varga, AK; Gerspach, J

Published in:
Molecular and Cellular Neuroscience

DOI:
10.1016/j.mcn.2004.05.008

ELSEVIER

MCN Molecular and Cellular Neuroscience

www.elsevier.com/locate/ymcne
Mol. Cell. Neurosci. 27 (2004) 215–226

Long-term NR2B expression in the cerebellum alters granule cell development and leads to NR2A down-regulation and motor deficits

Katalin Schlett,[a,b,1] Isabelle Pieri,[a,1] Friedrich Metzger,[c] Lara Marchetti,[a] Frank Steigerwald,[d] Ekrem Dere,[e] Dániel Kirilly,[b] Krisztián Tárnok,[b] Brigitta Barabás,[b] Ágnes Kis Varga,[f] Jeannette Gerspach,[a] Joseph P. Huston,[e] Klaus Pfizenmaier,[a] Georg Köhr,[d] and Ulrich L.M. Eisel[a,g,*]

[a]*Institute of Cell Biology and Immunology, University of Stuttgart, D-70569 Stuttgart, Germany*
[b]*Department of Physiology and Neurobiology, Eötvös Loránd University, H-1117 Budapest, Hungary*
[c]*Anatomisches Institut I, Universität Freiburg, 79104 Freiburg, Germany*
[d]*Department of Molecular Neurobiology, Max-Planck-Institute for Medical Research, D-69120 Heidelberg, Germany*
[e]*Institute of Physiological Psychology, University of Düsseldorf, D-40225 Düsseldorf, Germany*
[f]*Department of Neuropharmacology, Gedeon Richter Pharmaceutical Ltd., H-1475 Budapest, Hungary*
[g]*Department of Molecular Neurobiology, Rijksuniversiteit Groningen, NL-9750 AA Haren, The Netherlands*

Received 12 March 2004; revised 30 April 2004; accepted 26 May 2004
Available online 18 September 2004

***N*-methyl-D-aspartate receptor (NMDAR) composition in granule cells changes characteristically during cerebellar development. To analyze the importance of NR2B replacement by NR2C and NR2A subunits until the end of the first month of age, we generated mice with lasting NR2B expression but deficiency for NR2C (NR2C-2B mice). Mutant phenotype was different from NR2C knock-out mice as loss of granule cells and morphological changes in NR2C/2B cerebellar architecture were already evident from the second postnatal week. Increased NR2B subunit levels led also to a gradual down-regulation of cerebellar NR2A levels, preceding the development of motor impairment in adult animals. Therefore, cerebellar NR2A is important for proper motor coordination and cannot be replaced by long-term expression of NR2B. Consequently, the physiological exchange of NMDA receptor subunits during cerebellar granule cell maturation is important for accurate postnatal development and function.**

Introduction

N-methyl-D-aspartate receptors (NMDARs) are assembled as heteromers consisting of NR1 and NR2 subunits with one gene encoding for different splice variants of the NR1 gene and four genes encoding the different NR2 subunits (NR2A-D) (Hollmann and Heinemann, 1994). Modulatory functions of NR3 subunits have been also described (Das et al., 1998; Matsuda et al., 2003). NMDARs are considered to be important for neuronal plasticity, learning, and development because of their high Ca^{2+} permeability and their function as coincidence detectors due to voltage-dependent Mg^{2+} block (Dingledine et al., 1999).

The cerebellum shows a unique NMDAR subunit expression pattern during postnatal development (Monyer et al., 1994; Watanabe et al., 1994). Perinatally and during the first 2 weeks of murine development, granule cells express NR1 and NR2B subunits, while NR2A expression starts after birth. NR2B is subsequently replaced by the NR2C subunit at around P14–21. NR2A and NR2C become the predominant subunits in adult granule cells, thereby affecting NMDAR properties (Cull-Candy et al., 2001; Dingledine et al., 1999; Hollmann and Heinemann, 1994). These sequences of events coincide with the time course of granule cell migration and the establishment of synaptic connections between granule cells and Purkinje cells (Contestabile, 2000; Hatten, 1999; Hirai and Launey, 2000). Therefore, the properties of NR2B-containing NMDARs might be required for the migratory granule cells and synapse formation, whereas NR2A- and/or NR2C-containing NMDARs in mature granule cells might be required to maintain stable synaptic connections.

Experiments addressing the role of NR2B subunit in postnatal cerebellar development were hindered by the fact that both the deletion of the NR2B subunit and deletion of the C-terminus of the NR2B subunit are perinatally lethal (Kutsuwada et al., 1996; Mori et al., 1998; Sprengel et al., 1998). The role of NR2A and NR2C

* Corresponding author. Department of Molecular Neurobiology, Rijksuniversiteit Groningen, Groningen, Kerklaan 30, P.O. Box 14, NL-9750 AA Haren, The Netherlands. Fax: +31 50 363 2331.
E-mail address: U.L.M.Eisel@biol.rug.nl (U.L.M. Eisel).
[1] These authors made equal contributions.
Available online on ScienceDirect (www.sciencedirect.com.)

1044-7431/$ - see front matter © 2004 Elsevier Inc. All rights reserved.
doi:10.1016/j.mcn.2004.05.008

subunits in cerebellar function were studied in NR2A and/or NR2C knock-out mice (Kadotani et al., 1996) and in mice lacking the intracellular C-termini of NR2A and/or NR2C (Rossi et al., 2002; Sprengel et al., 1998). Despite the fact that granule cells express most of the NR2A and NR2C protein and are the major cell type in the cerebellum, absence of NR2A or NR2C caused either no or only minor changes in motor behavior while the electrophysiological properties of granule cells were noticeably altered (Ebralidze et al., 1996; Takahashi et al., 1996). NR2A/C double knock-out mice and mutants with deleted C-termini of NR2A and/or NR2C, on the other hand, showed reduced motor performance (Kadotani et al., 1996; Sprengel et al., 1998). The contribution of NR2A in motor coordination could be more important than that of NR2C since mice with C-terminally truncated NR2A subunits were more impaired than NR2C knock-out mice (Sprengel et al., 1998).

To understand the importance of the switch of NMDAR subunits during postnatal cerebellar development, we used a gene targeting strategy to replace NR2C by NR2B subunit in the murine cerebellum (designated NR2C-2B mice) to perpetuate a NMDAR configuration found in an earlier stage of granule cell maturation. Homozygous NR2C-2B mice express the NR2B subunit continuously in cerebellar granule cells and do not switch to NR2C, leading to a double phenotype of NR2C deletion and long-term presence of NR2B. The consecutive changes in cerebellar anatomy and motor coordination behavior in young and adult NR2C-2B mice together with compensatory alterations in other NMDAR subunit levels were analyzed.

Results

NR2C-2B mice express NR2B instead of NR2C in cerebellar granule cells

Using gene targeting, we have inserted a cDNA encoding the NR2B NMDAR subunit directly behind the ATG codon of the NR2C gene (Fig. 1A) and replaced the signal sequence of the NR2C gene. Murine embryonic stem cells carrying the mutation

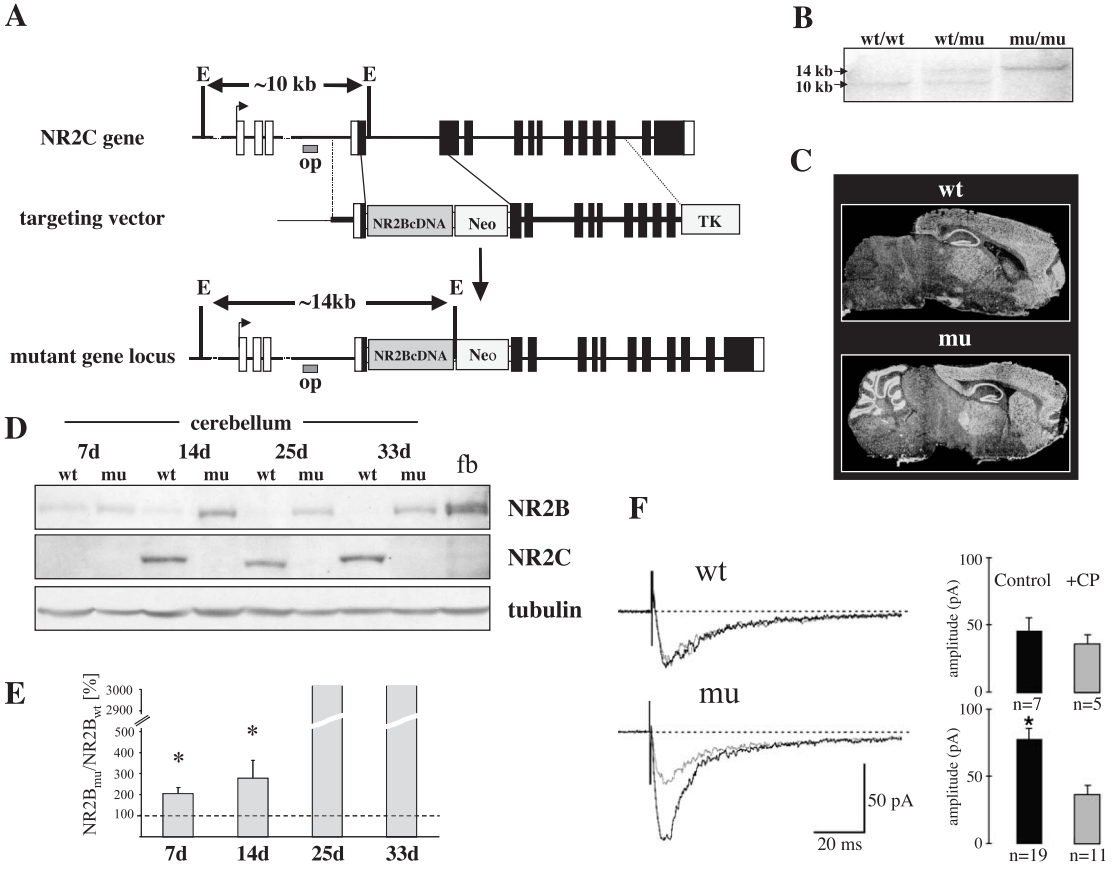

Fig. 1. NR2C-2B knock-in gene targeting strategy, genotyping, and expression analysis. (A) Structure of the murine NR2C gene locus, the knock-in gene targeting construct, and the mutated gene locus. Neo: neomycin resistance, TK: herpes simplex virus thymidine kinase. The mutated NR2C-2B gene locus can be identified through hybridization of a 14-kb *Eco*RI (E) band detectable in genomic Southern (B) using a 5′ outside probe (op). (C) In situ hybridization for the NR2B mRNA in brain sections prepared from 35-day-old wild-type (wt) and homozygous NR2C-2B (mu) mice. (D) Detection of NR2B and NR2C subunits in cerebellar lysates of wild-type (wt) and homozygous (mu) NR2C-2B animals at the age of 7, 14, 25, and 33 days. βIII-tubulin immunoblot shows the level of protein loaded in the lanes; fb: forebrain control. (E) NR2B protein levels in the cerebellum of NR2C-2B animals shown as percentage of densitometric values measured in wild-type animals at 7, 14, 25, and 33 days of age, respectively. Relative values were averaged from three independent Western blots and are shown as mean and SD. Dotted line indicates wild-type detection levels (100% relative density). (F) Left panels: NMDA EPSCs evoked by mossy fiber stimulation in acute cerebellar slices of both genotypes (P25), recorded in granule cells in 10 μM NBQX, 10 μM bicuculline (BIC) at −70 mV (Mg^{2+} was reduced) in the absence of CP-101,606 (black traces), and following perfusion of CP-101,606 (10 μM, 20 min; grey traces). Right panels: Averages of NMDA EPSC amplitudes of both genotypes in absence (control, black bars) and presence of CP-101,606 (+CP, grey bars). *$P < 0.05$ when compared with control NMDA EPSC of wild-type or $P < 0.006$ when compared with +CP of the mutant.

were injected into blastocysts of C57Bl/6 mice and chimeric animals were generated. Chimeras were bred in C57Bl/6 to homozygosity (Fig. 1B). First we performed in situ hybridization in 35-day-old mice to investigate the exchange of the NR2C by the NR2B subunit on the mRNA level (Fig. 1C). At this age, NR2B expression was detected in cerebellar granule cells of homozygous NR2C-2B but no longer in wild-type mice.

Western blot analysis of cerebellar tissue at different developmental stages also conferred the successful subunit exchange (Fig. 1D). NR2C protein in wild-type cerebella was detected from as early as P8 (data not shown) and high NR2C levels were evident by P14. On the other hand, NR2C was never detected in homozygous NR2C-2B mice, illustrating the complete lack of NR2C subunit protein. NR2B subunit levels were also compared by Western blotting (Figs. 1D and E). While NR2B disappeared from wild-type cerebella after the third postnatal week, homozygous NR2C-2B mice continuously expressed NR2B subunits (Fig. 1D). NR2B expression was not altered after Cre-mediated deletion of the floxed neomycin resistance gene, which was inserted downstream of the inserted NR2B cDNA cassette, by crossing the NR2C-2B mice with Cre-deleter mice (data not shown). This rules out that presence of the neomycin cassette reduces the expression of NR2B.

The time-course of NR2B subunit levels was investigated during the first month by densitometric analysis of four independent Western blots. The density of NR2B bands was normalized to the corresponding tubulin values, and quotients were compared with age-matched wild-type values (Fig. 1E). A 2- and a 2.5-fold elevation in mutant cerebellar NR2B subunit levels was already evident at P7 and P14, respectively, indicating NR2B expression from both mutant and the endogenous NR2B gene locus. As NR2B was not detectable in wild-type cerebella from the third postnatal week, relative NR2B levels were almost infinitely (>300 fold) increased at P25 and P33.

To demonstrate that NR2B is functional in mature cerebellar granule cells of NR2C-2B but not of wild-type mice, we recorded NMDA receptor-mediated excitatory postsynaptic currents (NMDA EPSCs) in acute slices prepared from wild-type and homozygous NR2C-2B mice older than 3 weeks (P22–P25). At this age, NR2B expression is developmentally down-regulated in wild-type mice (see, e.g., Takahashi et al., 1996) and the NR2B-specific antagonist CP-101,606 no longer affects NMDA EPSCs (Rumbaugh and Vicini, 1999). NMDA EPSCs were recorded at −70 mV in the presence of the AMPA receptor antagonist NBQX and were larger in NR2C-2B compared to wild-type mice (Fig. 1F, black traces, $P < 0.05$). As expected, perfusion of 10 μM CP-101,606 reduced NMDA EPSCs in NR2C-2B mice but was ineffective in wild-type recordings (Fig. 1F, grey traces, $P < 0.006$). Thus, NR2B-containing NMDARs contribute to synaptic NMDAR-mediated currents in NR2C-2B but not in wild-type mice older than 3 weeks.

Reduced granule cell number in NR2C-2B mice

The subunit exchange did not cause any gross alterations in the overall morphological brain structure of NR2C-2B mice (Fig. 1C). To investigate potential consequences of prolonged NR2B expression on the cellular level, we investigated histological cerebellar sections during postnatal development of wild-type and NR2C-2B mice. The thickness of the external and internal granule cell layers (EGL and IGL, respectively) and the molecular layer (MOL) was measured in midsagittal sections of the vermal region, in the same location of three cerebellar lobules (lobules 3, 4/5, and 8). Data derived from different lobules were consistent; the results obtained from lobule 4/5 are shown in Fig. 2.

The thickness of the EGL was slightly, but not significantly, increased during the first 2 weeks of age (P7: WT = 47.2 ± 7.9 μm, NR2C-2B = 50.4 ± 8.1 μm; P10: WT = 28.8 ± 4.1 μm,

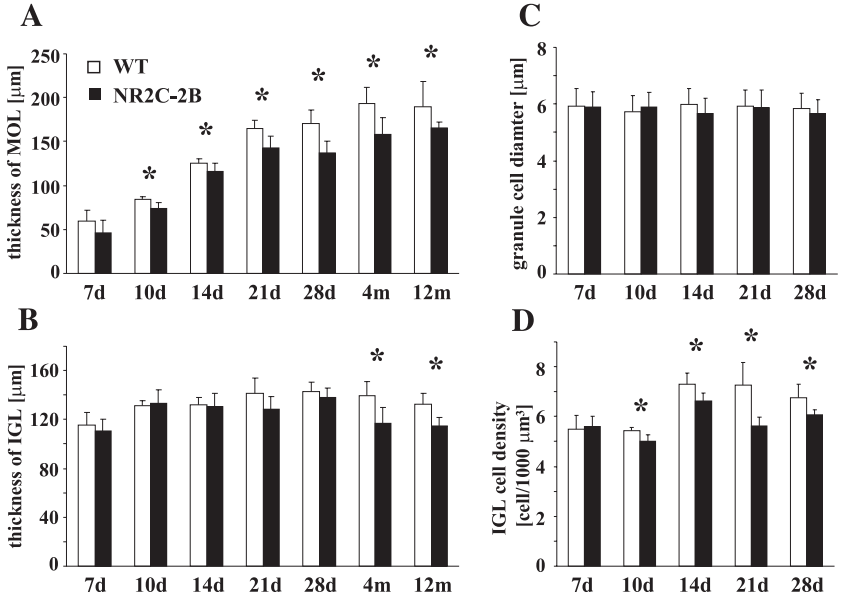

Fig. 2. Altered cerebellar layer development in NR2C-2B mice. (A and B) Comparison of the thickness of the molecular layer (MOL; A) and internal granule layers (IGL; B) in lobule 4/5 during postnatal development (7, 10, 14, 21, 28 days, 4 and 12 months of age) in wild-type (WT) and NR2C-2B mice. (C and D) The average granule cell diameter (C) did not differ during the postnatal development of wild-type and NR2C-2B cerebella but granule cell density (D) was markedly reduced between P10 and P28, indicating reduced granule cell number in NR2C-2B mice older than P10 (*$P < 0.05$).

NR2C-2B = 33.3 ± 3.0 μm; P14: WT = 10.8 ± 3.4 μm, NR2C-2B = 11.4 ± 1.0 μm). Since wild-type and NR2C-2B granule cells disappeared from the EGL approximately at the same time, migratory period itself was not profoundly prolonged. MOL was significantly reduced in NR2C-2B mice at P10, and this difference persisted until adulthood (Fig. 2A). IGL thickness was significantly reduced in adult NR2C-2B mice with a similar tendency at P21 and P28 (Fig. 2B). Average cell density and cell diameter were also measured during postnatal cerebellar development. Granule cell diameter was similar between mutant and wild-type animals and did not change at any of the investigated ages (Fig. 2C). Cell density, on the other hand, was significantly reduced in mutant animals between P10 and P28 (Fig. 2D). Therefore, the number of granule cells located in the IGL of the mutant animals was already reduced at P10 and remained reduced throughout life.

To find out whether the reduced number of granule cells is due to the overexpression of NR2B or to the lack of NR2C, histology was also carried out in NR2C knock-out mice (Kadotani et al., 1996; Sprengel et al., 1998), which did not indicate any gross changes in adult cerebellar architecture. No data were available, however, from young postnatal ages; therefore, we investigated layer thickness from P8 and P16, at time points when the thickness of the MOL started to change in NR2C-2B mice (Fig. 2A). At P8, no differences in layer thickness were revealed in NR2C-2B or NR2C knock-out mice compared to wild-type littermates (Table 1). At P16, however, MOL thickness was already reduced in NR2C-2B but not in NR2C knock-out mice (Table 1). Thus, the reduced number of granule cells in young NR2C-2B mice cannot be explained by the lack of NR2C and must be a consequence of early NR2B overexpression.

Impaired granule cell migration in cerebella from NR2C-2B mice in vitro

The reduced number of granule cell number observed after P10 in NR2C-2B mice may be due to increased cell death, reduced proliferation, or migratory deficits of granule cells. To address these possibilities, NR2C-2B mice were investigated at developmental ages when the migratory activity of granule cells decreases from a high to a low level (Komuro and Rakic, 1995; Komuro et al., 2001), in the cerebellar brain sections of P8 and P16 NR2C-2B mice and in organotypic cerebellar slice cultures prepared from P8 mice.

TUNEL staining and BrdU labeling did not reveal any evident alterations in brain sections or in organotypic slice cultures of NR2C-2B mice compared to wild-type littermates (data not shown). To reveal differences in the migratory behavior of NR2C-2B granule cells compared to wild-type, TAG-1 immunohistochemistry was performed. Young postmitotic granule neurons located in the inner part of the EGL, the postmitotic zone (pmz), express the axonal glycoprotein TAG-1 (Furley et al., 1990, Solecki et al., 2001). This marker, therefore, identifies parallel fibers and axons of granule cells that initiate migration through the molecular layer (MOL). Overall staining pattern was similar between mutant and wild-type brain sections: at P8, strong TAG-1 immunoreactivity was detected in the pmz of the EGL (see Table 1) and some fibers parallel to Bergmann glia cells were also stained. By P16, TAG-1-positive cells disappeared in both mutant and wild-type animals (data not shown).

We attempted to compare TAG-1 staining patterns between wild-type and mutant littermates at P8; therefore, the thickness of strongly TAG-1 immunopositive layers in the pmz containing premigratory granule cells and parallel fibers was measured (Table 1). Using the same criteria for analyzing the pictures, significant differences were not revealed between wild-type and mutant littermates, neither in NR2C-2B nor in NR2C knock-out mice.

As a more detailed quantification of staining patterns in brain slices was not possible, organotypic cerebellar slice cultures of both genotypes were investigated. It has been shown that Purkinje cells as well as granule cells develop in a well-characterized way when cultivated in organotypic slice cultures from P8 mouse cerebellum for up to 12 days in vitro (DIV) (Adcock et al., 2004; Schrenk et al., 2002; for a review, see Metzger and Kapfhammer, 2003; Seil, 1996). The major advantage of this culture system is that it allows a more detailed, quantitative analysis of in vitro granule cell migration and development (Kunimoto and Suzuki, 1997; Tanaka et al., 1994).

In wild-type organotypic slices, TAG-1 expression appeared very strong until about DIV 6 and subsequently decreased until DIV 12 when TAG-1 immunosignals were found in only 25% of all wild-type slices, indicating the end of granule cell migration (Figs. 3A and C). In contrast, 85% of identically treated slice cultures from NR2C-2B mice still contained many TAG-1 fibers at DIV 12, which were mostly orientated radially (Fig. 3B). Comparing the average number of TAG-1-positive fibers in the slices, significantly less fibers were stained in slices from wild-type than from NR2C-2B mice ($P < 0.001$; Fig. 3D).

We also employed an antibody against NeuN, which exclusively stains postmitotic granule cell bodies and nuclei in the cerebellum. Organotypic cultures from the central vermis, where the overall structure of the cerebellum is best preserved, were

Table 1
Thickness of cerebellar layers and TAG-1-positive zones in 8- and 16-day-old (P8 and P16, respectively) NR2C-2B and NR2C knock-out animals, measured in midsagittal sections of the vermal region, in the same location of three cerebellar lobules (lobules 3, 4/5, and 9)

Mouse line		P8				P16	
		EGL	TAG-1 positivity	MOL	IGL	MOL	IGL
NR2C-2B	wt	46.3 ± 4.2	28.4 ± 2.9	96.8 ± 8.6	113.4 ± 8.4	194.7 ± 20.7	119.6 ± 12.5
	mutant	42.7 ± 4.9	28.7 ± 4.8	93.3 ± 6.5	114.3 ± 6.5	158.7 ± 16.7***	113.9 ± 8.6
NR2C k.o.	wt	43.8 ± 4.5	33.5 ± 5.8	101.9 ± 9.1	137.2 ± 9.7	194.1 ± 34.4	146.2 ± 16.03
	k.o.	40.4 ± 3.7	34.6 ± 4.1	106.4 ± 7.2	133.7 ± 5.8	175.6 ± 18.8	159.2 ± 9.75

Data derived from different lobules were consistent; the results obtained from lobule 9 are shown. Data were compared between littermates from the same mouse line; values are displayed in μm and represent mean ± SD. Significant reduction in the thickness of MOL was found only in NR2C-2B mutant animals at the age of postnatal day 16.
*** $P < 0.001$.

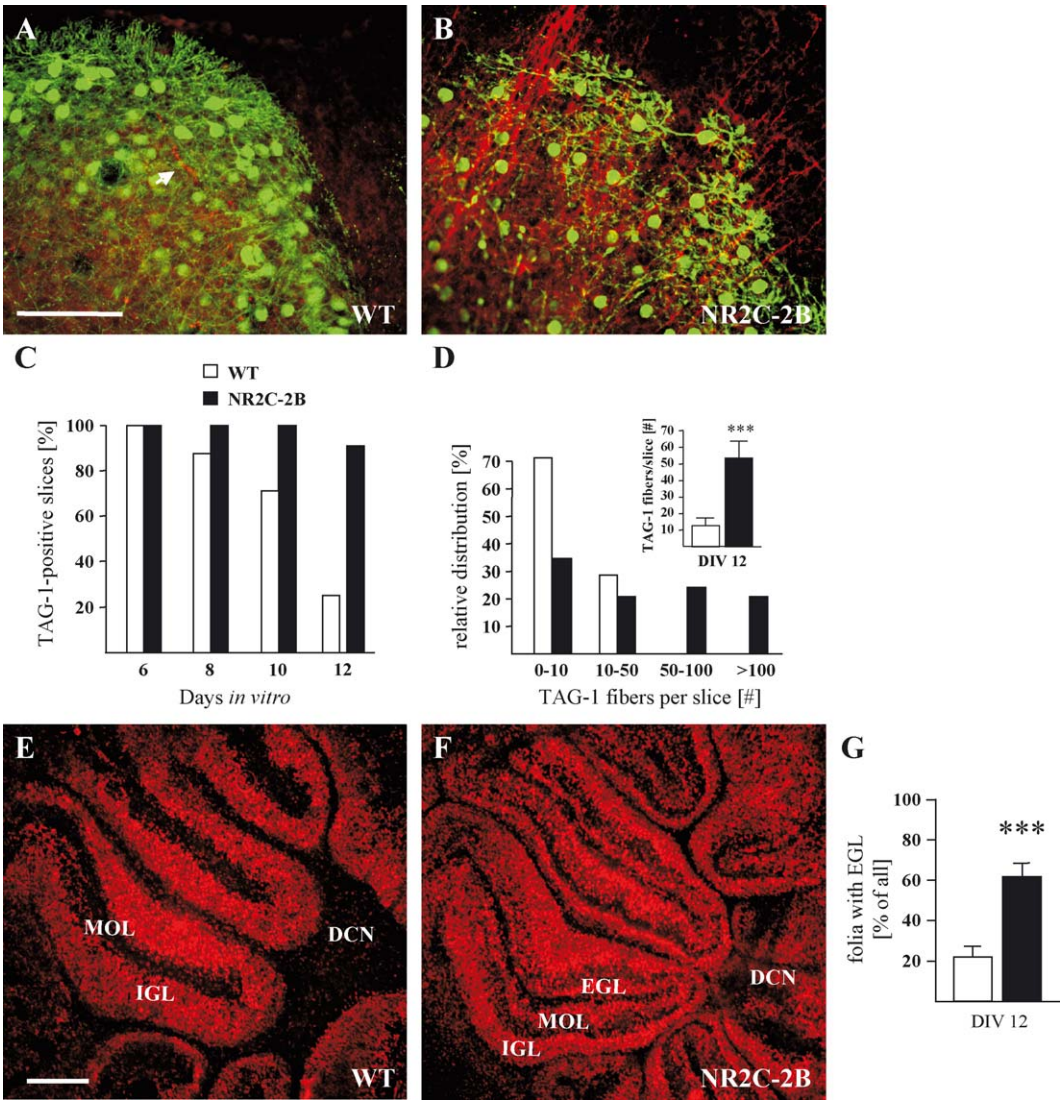

Fig. 3. Altered granule cell migration in cerebellar slice cultures from NR2C-2B mice. (A and B) Comparison of cerebellar slice cultures (DIV12) prepared from P8 wild-type (WT) and NR2C-2B mice following immunostaining against TAG-1 (red) and Calbindin D-28K (green). Note the higher number and radial orientation of TAG-1 fibers in NR2C-2B slice cultures. (C) Time course of TAG-1 staining in cerebellar slice cultures. (D) Histogram showing the number of TAG-1 fibers per slice. The inset shows the average number of TAG-1-positive fibers per slice (***$P < 0.001$, unpaired t test). Data represent mean ± SEM of 7 WT and 29 NR2C-2B slices from four independent experiments. (E and F) NeuN staining (red) indicated the presence of an EGL in cerebellar slice cultures (DIV12) of NR2C-2B but not in wild-type mice. (G) Quantification of NeuN staining (***$P < 0.001$, unpaired t test). Data represent mean ± SEM of 28 and 32 slices investigated from four and five independent experiments in WT and NR2C-2B mice, respectively. EGL, external granule cell layer; MOL, molecular layer; IGL, internal granule cell layer; DCN, deep cerebellar nucleus. Scale bars are 50 μm in A and 250 μm in E.

analyzed at DIV 12. At this age, NeuN-positive EGLs were found only in very few wild-type cultures, as granule cell migration seemed to be concluded (Fig. 3E). By contrast, significantly more folia from NR2C-2B cerebella (Fig. 3G) still contained NeuN-positive EGL ($P < 0.001$; Fig. 3F). These in vitro results suggest a subtle deficit during the migration of NR2C-2B granule cells that could contribute to the observed loss of granule cells.

Purkinje cells in NR2C-2B mice receive a reduced number of excitatory synaptic inputs

Reduced number of granule cells in NR2C-2B mice and therefore the reduced number of parallel fibers could decrease the number of synapses between granule cells and Purkinje cells. As cerebellar synaptic connections show high plasticity during development (Ito, 1984; Palay and Chan-Palay, 1974), serial electron microscopic pictures were taken throughout the molecular layer of lobule 10 from wild-type and NR2C-2B mice at a developmental age when synaptic connections are already stabilized (Fig. 4). In the recorded pictures, we were unable to make a clear distinction between climbing fiber and parallel fiber synapses on dendritic spines of Purkinje cells based only on their morphology. However, parallel fibers more frequently end on dendritic spines of Purkinje cells than climbing fibers (Ito, 1984; Palay and Chan-Palay, 1974). Therefore, we counted all synapses ending on dendritic spines and regarded them as excitatory synapses, provided that both presynaptic vesicles and the postsynaptic density were clearly visible (see Figs. 4A and B).

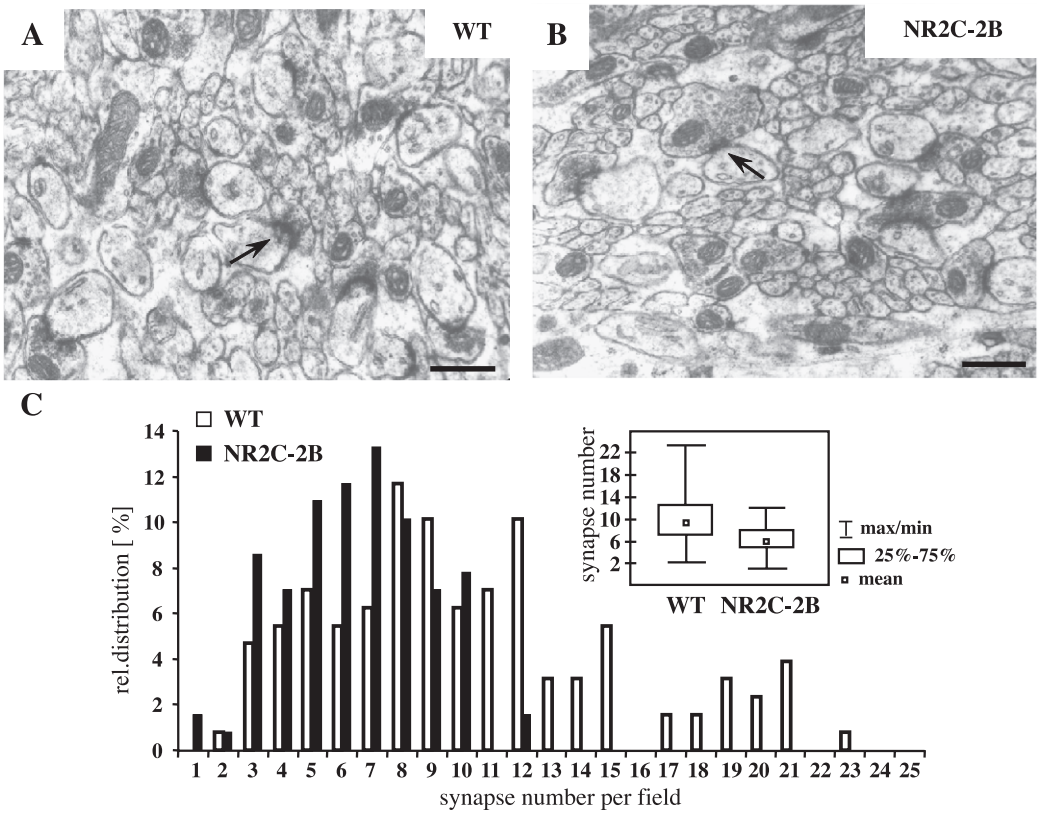

Fig. 4. The number of excitatory synapses on Purkinje cell dendrites is reduced in NR2C-2B mice. Synapses ending on Purkinje cell dendritic spines recorded from the molecular layer in lobule 10 of wild-type (A) or NR2C-2B (B) animals. (C) The number of synapses between excitatory fibers and Purkinje cell dendritic spines was determined on each recorded field (31 μm^2; ANOVA; $P < 0.0001$; arrows indicate examples). Scale bars indicate 0.4 μm.

One hundred twenty-eight and 103 electron microscopic pictures were analyzed from three wild-type and three NR2C-2B animals at 3 months of age.

Ultrastructural analyses did not reveal any morphological difference in shape or size between wild-type and NR2C-2B excitatory synapses (Figs. 4A and B). For a semiquantitative analysis, the relative distribution of the excitatory synapses per recorded field (31 μm^2) was compared between wild-type and NR2C-2B animals (Fig. 4C). Mean synapse number was reduced by about one third in NR2C-2B mice (10.23 ± 4.89 versus 6.41 ± 2.38 synapses/field), and there was a significant reduction in the relative frequency of fields with high synapse numbers ($P < 0.0001$). Taken together, the subunit exchange led to a reduced number of granule cells and to a reduced number of excitatory synapses counted on Purkinje cell dendrites in adult mutant animals.

Adult NR2C-2B mice exhibit deficits in motor coordination

To find out if altered NMDAR subunit composition and/or changes in the cerebellar morphology have consequences on motor behavior, young and adult NR2C-2B mice were investigated for their performance on a fixed speed and an accelerating rotarod. During fixed speed rotarod tests, mice were placed onto a 20-mm diameter rod revolving at 12 rpm and the time animals could stay on the rod was measured on three consecutive days (Figs. 5A–C). Motor deficits in NR2C-2B mice compared to age-matched wild-type animals gradually increased with age. No difference was found at 3 months of age, but 6-month-old mutants already performed slightly, but not significantly, worse than wild-type animals. One-year-old mutant animals, on the other hand, could never reach up to the performance of control mice even though their performance improved after repeated trainings.

The more challenging accelerating rotarod test (speeding up to 40 rpm) was also used. The time 3- to 4-week-old animals stayed on the accelerating rod significantly increased from trial to trial at each of three consecutive days in both NR2C-2B and wild-type littermates, but motor performance was not significantly different at this age (Fig. 5D). At 4 months of age, on the other hand, differences were already evident (Fig. 5E). Whereas wild-type animals did not show an improvement in performance, probably due to a ceiling effect, NR2C-2B mice remained for a significantly shorter time on the accelerating rod than controls during the first 2 days ($P < 0.05$; Fig. 5E). Mutant mice could improve their performance with each trial and reached wild-type level at the third trial of the first 2 days and at all trials of the third day of testing.

To summarize, despite early morphological changes in the cerebellar architecture of NR2C-2B mice, young mutants were not impaired in motor coordination. Motor deficits in NR2C-2B mice became evident by 4 months and increased with age.

Age-dependent reduction of NR2A levels in NR2C-2B mice

To investigate if persisting NR2B expression in NR2C-2B mice affects endogenous NMDA receptor subunit levels, Western blot analyses of cerebellar lysates from NR2C-2B and wild-type

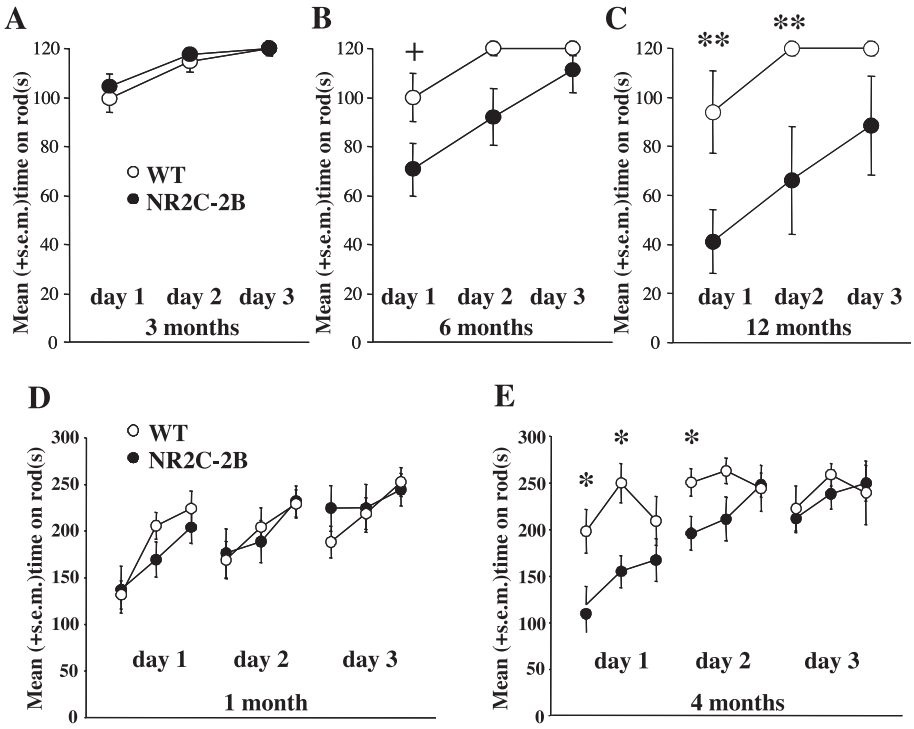

Fig. 5. Motor coordination deficits are found only in adult NR2C-2B mice. Circles represent the mean (+SEM) time the animals remained either on the fixed speed (A–C) or on the accelerating rotarod (D and E). $^{**}P < 0.001$; $^{*}P < 0.05$ (NR2C-2B versus wild-type).

mice at the age of 2 weeks, 1, 2, 3, 4, 5, and 12 months were performed (Figs. 6A and B). Detection of NR1, NR2A, NR2B, and NR2C subunits at each developmental age was repeated 3–9 times, and subunit levels normalized to the corresponding tubulin values were compared between age-matched mutant and wild-type samples. In agreement with the double phenotype of NR2C-2B mice, relative NR2B subunit levels were highly up-regulated while NR2C was absent in mutant cerebellar samples at all developmental ages. NR1 levels were similar between wild-type and NR2C-2B cerebella. Relative NR2A levels in mutant samples, on the other hand, were slightly reduced between the first and third month of age but significantly reduced after the fourth month of age.

As NR2B disappeared from wild-type cerebellum after the second postnatal week (Fig. 1D), changes in mutant NR2B subunit levels during development were revealed by comparing normalized density values from older NR2C-2B cerebellar samples to the values detected in P14 mutant samples (Figs. 6C and E). Experiments were repeated three times independently. Mutant NR2B expression was gradually decreased after the second month of age; but in contrast to the almost complete elimination of NR2A (Figs. 6A and B), NR2B was still strongly detected in the cerebellum of aged mutant mice (Figs. 6C and E).

To rule out the possibility that the lack of NR2C in NR2C-2B mutants could be responsible for the observed alterations in NR2A levels, Western blot analyses were also performed with cerebellar extracts prepared from NR2C knock-out animals (Figs. 6D and F). $NR2C^{-/-}$ phenotype was clearly indicated by the lack of NR2C in knock-out cerebellar extracts. Importantly, no differences in NR2A levels were found between wild-type and NR2C knock-out samples even at 5 months of age (Fig. 6E). Therefore, reduced NR2A levels in NR2C-2B animals must be a consequence of long-term NR2B expression in cerebellar granule cells.

Discussion

NR2B expression is tightly regulated and determines important NMDAR functions during brain development (Cull-Candy et al., 2001), which is best illustrated by the lethal phenotype following inactivation of the NR2B gene (Kutsuwada et al., 1996). In murine cerebellar granule cells, NR2B expression is restricted to the first three postnatal weeks and is subsequently replaced by the NR2C subunit. Our data show that developmental down-regulation of NR2B and replacement by NR2C in granule cells is functionally important. We approached this issue by a knock-in gene targeting strategy, replacing the coding region of the NR2C gene by NR2B, thereby bringing NR2B under the control of the NR2C promoter and thus deleting the developmental switch from NR2B to NR2C.

Mutant phenotype became evident by the end of the first postnatal week as elevated NR2B levels were found in cerebellar tissue at P7. Although NR2C subunit protein was not detected in wild-type cerebellum before P8, low NR2C mRNA expression was reported in the external granule cell layer (EGL) at P3 and P14 in rats (Akazawa et al., 1994) and at P1 and P7 in mice (Watanabe et al., 1994). Therefore, we conclude that NR2B expression from the mutant gene locus could already start in the premigratory granule cells of the EGL during the first postnatal week.

Histological alterations, observed in NR2C-2B mice older than 10 days, could be the consequence of the constitutive expression of NR2B and/or absence of NR2C in granule cells. In NR2C knock-out mice, cerebellar histology and the overall morphological properties of cerebellar granule cells appeared normal in young and adult mutants (see our results and Kadotani et al., 1996, respectively). Thus, reduced number of granule cells and decreased thickness of the molecular layer in NR2C-2B mice are most likely due to the constitutive NR2B expression and not to the lack of NR2C.

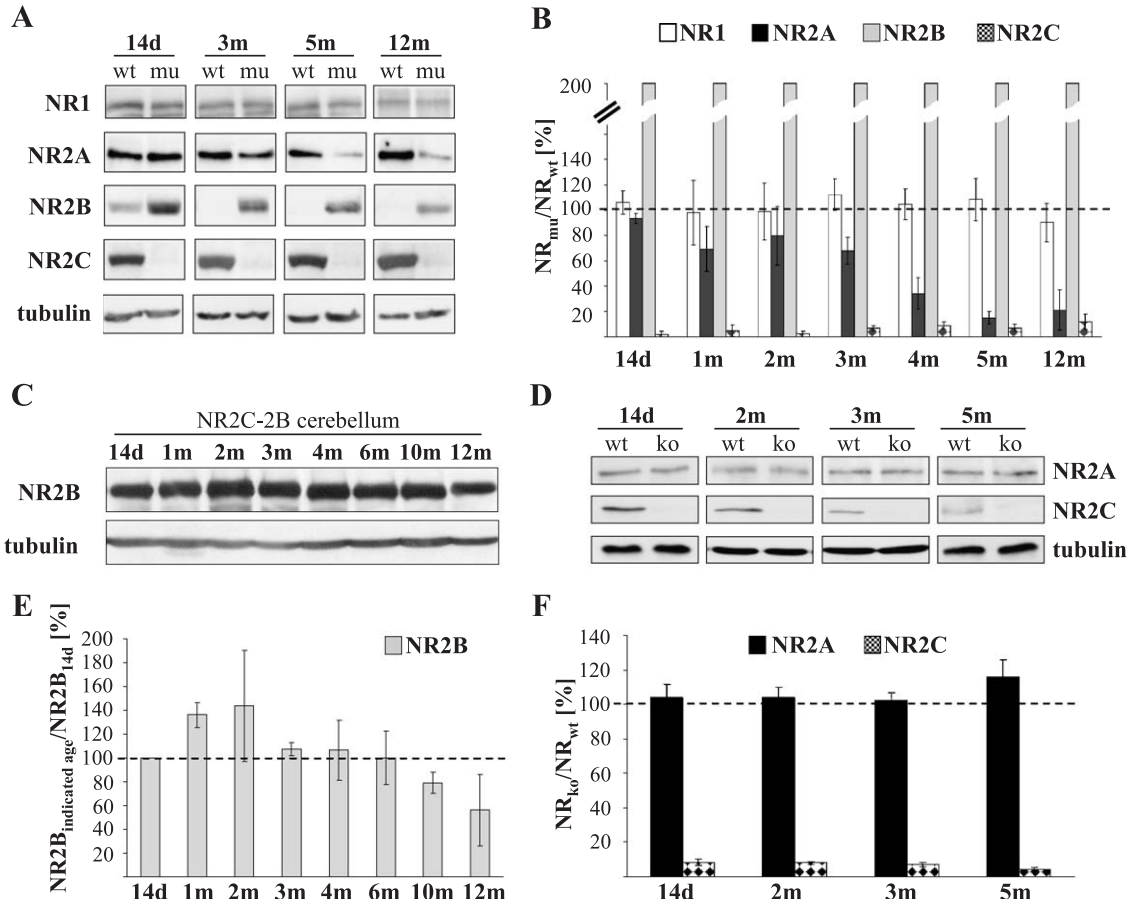

Fig. 6. Age-dependent changes in NMDA receptor subunit levels in NR2C-2B (A–C, E) and NR2C knock-out (D and F) mice. (A) Representative Western blotting analyses of NR1 and NR2A, NR2B, and NR2C levels in cerebellar extracts from wild-type (wt) and NR2C-2B (mu) mice at 14 days, 3, 5, and 12 months of age. (B) Densitometric quantification of relative subunit levels in NR2C-2B cerebella at 14 days and 1, 2, 3, 4, 5, and 12 months of age, compared to age-matched wild-type levels. (C and E) Representative Western blot and densitometric analyses of NR2B levels in NR2C-2B cerebellar extracts during postnatal development. (D and F) NR2A and NR2C levels in cerebellar extracts of NR2C knock-out and wild-type littermates during development. In the graphs, relative values are obtained from three to five independent Western blots and shown as mean ± SD. Dotted lines indicate 100% subunit level of age-matched wild-type animals (B and F) or NR2B expression in P14 NR2C-2B cerebellum (E).

Our histological analyses showed a significant decrease in granule cell number in the internal granule cell layer (IGL) starting from P10. Theoretically, three possibilities can be considered to contribute to the early loss of granule cells: effects on cell proliferation, cell death, and/or cell migration. Recent evidence suggests that NMDARs may have promoting effects on neuronal precursor proliferation (Luk et al., 2003), and functional NMDARs were detected in the EGL before migration (Farrant et al., 1994; Rossi and Slater, 1993). It is unlikely, however, that the proliferation of granule cell precursors in NR2C-2B mice was severely reduced by altered NMDAR subunit composition as the thickness of EGL was slightly increased, and in vivo BrdU labeling of proliferating cells did not reveal differences between wild-type and mutant animals.

NMDARs influence granule cell migration from the EGL to the IGL (Komuro and Rakic, 1993), and our TAG-1 and NeuN staining in organotypic cultures supported a transient impairment of granule cell migration. Thus, migratory deficit could contribute to reduce the number of granule cells in vivo. Alternatively, increased amount of NR2B subunits in the NMDARs may cause overexcitation and, consequently, excitatory cell death (Bessho et al., 1994; Marshall et al., 2003), which could affect premigratory and migrating granule cells in NR2C-2B mice since the activation of NR2C promoter already starts in the EGL (Akazawa et al., 1994; Watanabe et al., 1994). Moreover, cell death could also occur in the IGL, in maturing granule cells, since the involvement of NR2B subunits in the synaptic NMDA receptors lead to significantly increased NMDAR currents in granule cells of NR2C-2B mice older than 3 weeks. Although TUNEL staining did not reveal major differences between wild-type and mutant cerebella, impaired NMDAR signaling in NR2C-2B mice via NR2B-containing NMDARs leading to cell death remains a possibility.

The number of granule cells and the thickness of the molecular layer were reduced to a similar level (10–20% reduction) in P10 and in adult cerebella, indicating that cell loss was already completed in young NR2C-2B mice. Cerebellar NR2A level, on the other hand, started to decrease only after 1 month of age (Fig. 6B) and was almost completely eliminated in mutants older than 5 months (80% reduction), indicating that the reduced number of granule cells cannot account for NR2A decline. The selective down-regulation of another NMDAR subunit may represent a compensation for the continuous NR2B expression to escape increased NMDAR signaling since both subunits confer similar

voltage dependence and single channel conductance to NMDARs (Cull-Candy et al., 2001; Dingledine et al., 1999). Down-regulation of NMDAR subunits or complexes upon overstimulation of granule cells has also been reported in other animal models (Brandoli et al., 2002; Liesi et al., 1999; Watanabe et al., 1998). NR2A down-regulation was previously shown to reduce excitotoxicity (Brandoli et al., 2002; Nabekura et al., 2002) and could play a similar role in NR2C-2B cerebella.

The number of granule cells affects the number of parallel fibers and consequently influences Purkinje cell innervations and development (Takács et al., 1997). Thus, the observed shrinkage in the thickness of MOL is in accordance with reduced number of parallel fibers originating from less granule cells. This explanation was confirmed by electron microscopic analyses showing that excitatory input to Purkinje cell dendrites was decreased in adult NR2C-2B mice, at a time point when large scale synaptic changes had already taken place (Palay and Chan-Palay, 1974; Takács and Hámori, 1994).

Cerebellar circuitry is important for motor coordination and behavior. Despite the fact that NMDARs in cerebellum influence motor coordination and plasticity (Hansel et al., 2001), it was found that neither the lack of NR2A nor the lack of NR2C alone leads to obvious motor coordination deficits. Motor coordination impairment was found only in adult NR2A/NR2C double knock-out mice on the fast rotarod (Kadotani et al., 1996). NR2C-2B mice did not show any motor deficits up to 3 months, although at this age the cellular architecture in mutant mice was already disturbed. Therefore, subtle migratory deficits and the reduction in granule cells of the IGL cannot be directly linked to the disturbed motor behavior of adult NR2C-2B mice.

At 4 months of age, NR2C-2B mutation led to a more severe motor coordination phenotype than the simple deletion of NR2C (Kadotani et al., 1996; Sprengel et al., 1998). The long-term presence of NR2B subunits in adult granule cells could directly influence motor behavior in NR2C-2B mice. Since motor coordination was not impaired in young animals, a more feasible explanation for impaired motor performance in NR2C-2B mice is provided by the severe decline in cerebellar NR2A levels after the third month of age, coinciding in time with the onset of motor impairment. NR2C is absent from mutant cerebella; therefore, reduced NR2A level together with the lack of NR2C can provide an explanation for the observed impaired motor coordination, resembling NR2A/NR2C double knock-out mice.

Taken together, our observations indicate that ongoing NR2B expression in cerebellar granule cells cannot functionally substitute for NR2C and leads to declining NR2A expression. Consequently, the natural exchange of the NR2B by the NR2C subunit in wild-type cerebellar granule cells is an important prerequisite of accurate cerebellar development and function.

Experimental methods

Targeting vector

A genomic clone containing the coding sequence of the *NR2C* gene was isolated from a mouse genomic library (Pieri et al., 1999). The 1.9-kb *Sac*I fragment of the clone 11, containing the exon 4 of the *NR2C* gene, was cloned into pBluescript SK+ to yield *pMK1*. The synthetic linker 5′ -cgatatccgggccctcgagaagcttgtcgacatcgatggtac-3′ was ligated with the Asp718–*Sac*I 2.9 kb fragment of pBluescript SK+ to yield *pUli3*. The *Apa*I–*Pvu*II fragment of *pMK1*, a 1.8-kb *Xho*I–*Hin*dIII fragment containing the *tk* gene driven by the *PGK* promoter and the 7-kb *Hin*dIII fragment isolated from the genomic clone 11 were successively cloned into *pUli3* to yield *pE3X3*. The 1.3-kb *Xho*I fragment of *pE3X3* was replaced by the synthetic linker 5′ -tcgattaattaagggggccggcc-3′ to yield *pE3X3AB*. The synthetic linker 5′ -gtaccttaattaaataatggccatctagagggttcgaagtcgacggggaattcaataagcttgcggccgcg-cgatcgcctcgagggcgccggc-3′ was ligated with the Asp718–*Sac*I 2.9 kb fragment of pBluescript SK+ to yield *p103*. The neomycin resistance gene driven by *PGK* promoter (flanked by lox sites) and the NR2B cDNA were cloned into the *Sgf*I–*Nar*I sites and *Sal*I–*Not*I sites of *p103*, respectively, to yield *pNeoloxE2*. Finally, the neomycin resistance gene, its flanking lox sites and the NR2B cDNA were subcloned into the *Pac*I–*Fse*I sites of *pE3X3AB* to yield the targeting vector *pE3E2neolox*.

Selection of ES cells, blastocyst injection, mouse breeding, and genotyping

RW4 cells (Genome Systems, USA) were cultured in Dulbecco's modified Eagle medium supplemented with 15% ES-FCS, nonessential amino acids (all Gibco BRL), 1000 U/ml recombinant LIF (ESGRO™), and 3 μM β-mercaptoethanol. Introduction of *Cla*I-cleaved targeting vector *pE3E2neolox* was done by electroporation using a BioRad Gene Pulser (25 μF, 0.4 KV). Selection was done with 350 μg/ml G418 (Gibco BRL) and 2μM gancyclovir (Roche Diagnostics). All animal procedures were performed according to German animal protection law. ES cells of recombinant subclones were injected into C57BL/6 blastocysts, subsequently transferred into pseudopregnant B6CBF1 females (RCC Ltd., Wüllinsdorf, Switzerland). Highly chimeric males were mated with C57BL/6 females to obtain F1 offsprings.

ES cell DNA was digested with *Hin*dIII and then analyzed on 0.7% agarose gels and tested by Southern blotting: DNA was transferred to nylon membrane (Qiagen) and hybridized using Quickhyb solution (Stratagene) with the 3′ external probe (see Figs. 1A and B) and the neo probe (pMC1). Membranes were washed in 0.2× SSC, 1% SDS twice at RT, then in 0.1× SSC, 1% SDS once at 60°C. For routine genotyping, DNA samples from mice were prepared from tails and genotypes were determined [by PCRs using the NeoA–NeoB primer set (which generates a 700-bp fragment) and the e3e2–e2a primer set (which generates a 260-bp fragment)] by digestion of DNA with *Eco*RI and analysis by hybridization as described above.

In situ hybridization

In situ hybridization was essentially performed as previously described (Klein et al., 1998). Briefly, whole brains were taken from mice and frozen on dry ice. Twenty-micrometer sections were cut using a Leica cryostat at −25°C, placed on silanized glass slides, fixed with 4% paraformaldehyde in PBS and stored in 70% ethanol at 4°C. Antisense ^{35}S-labeled probes were prepared from linearized templates using the T3/T7 in vitro transcription system (Ambion, Austin, TX, USA). Sense transcripts were used as controls. Hybridized slides were dipped with LM-1 photo emulsion (Amersham-Pharmacia, Germany) following exposition for 2 weeks at 4°C. Slides were developed according to the manufacturers recommendations and analyzed in dark field microscopy.

Western blot analysis

Cerebellar and forebrain protein extracts were prepared by homogenization in 8–10 volumes of ice-cold buffer containing 0.32 M sucrose, 1 mM $NaHCO_3$, 1 mM $MgCl_2$, 0.5 mM $CaCl_2$, and protease inhibitors (0.5 mM phenylmethylsulfonylfluoride, 10 μg/ml leupeptine, 2 μg/ml aprotinin, and 10 μM bestatin), using a Potter homogenizer with 12 strokes at 800 rpm. Brain homogenates were centrifuged at 1400 × *g* for 10 min at 4°C, and supernatants were used for Western blot analysis. Protein content of the samples was determined using the BioRad Bradford reagent (BioRad, Germany). Fifty micrograms protein per lane were loaded, separated by 7.5% SDS-PAGE and transferred onto nitrocellulose membrane (Hybond ECL extra, Amersham, Germany). Primary antibodies were used overnight at +4°C as follows: anti-NR1 (rabbit, 1:500, Chemicon, Temecula, CA), anti-NR2A (rabbit, 1:3000, Upstate Biotech, Lake Placid, NY), anti-NR2B (BM 1B3.3B6, mouse, 1:10,000; Laurie et al., 1997), anti-NR2C (rabbit, 1:1000, Chemicon, Temecula, CA), and anti-βIII-tubulin (TUJ1, mouse, 1:5000, BAbCo, Richmond, CA). Blots were further incubated with anti-rabbit or anti-mouse IgGs conjugated with horse radish peroxidase (Pierce, Rockford, USA) at a dilution of 1:10,000 for 1 h. Antibody binding was visualized using the ECL chemiluminescence detection system (Amersham).

Densitometric quantifications of NR1 and NR2 subunit levels were performed using TINA2.09 g (Seescan Ltd., USA) and TotalLab (Nonlinear Dinamics Ltd., USA) softwares. In each sample, NMDA receptor subunit densities were first normalized to the corresponding βIII-tubulin densities, then quotients were compared to the quotients obtained from age-matched wild-type cerebellar samples or from a reference sample on the same blot. Relative subunit levels were averaged from the independent densitometric analyses of three to nine individual Western blots from each developmental age.

Electrophysiology

Granule cells were identified in acute cerebellar slices (250 μm) of wild-type and homozygous NR2C-2B mice (P22–25) by infrared differential interference contrast microscopy (Stuart et al., 1993) and were voltage clamped using an EPC-9 amplifier (HEKA elektronik, Germany). The extracellular solution contained (in mM) 125 NaCl, 2.5 KCl, 25 Glucose, 25 $NaHCO_3$, 1.25 NaH_2PO_4, 2 $CaCl_2$, 0.1 $MgCl_2$, 0.01 bicuculline (BIC, Sigma) a $GABA_A$ receptor blocker, 0.01 NBQX (Tocris) a AMPA receptor antagonist, and 0.01 glycine (Sigma) the NMDAR coagonist, continuously bubbled with 5% CO_2/95% O_2. The intracellular solution contained (in mM) 110 Cs-gluconate, 20 CsCl, 10 NaCl, 10 HEPES, 0.2 EGTA, 4 ATP-Mg, 0.3 GTP-Na, and 2.5 QX-314 (Calbiochem, La Jolla, CA), a sodium channel blocker (pH 7.25, CsOH). Pipette resistance was between 5 and 7 MΩ. The cell properties were deduced according to D'Angelo et al. (1995) and were similar in wild-type and NR2C-2B mice (input resistance: WT, 2.3 ± 0.3 GΩ, n = 13, and NR2C-2B mice, 2.2 ± 0.2 GΩ, n = 24; membrane capacitance: WT, 4 ± 0.4 pF, n = 13, and NR2C-2B mice, 3.8 ± 0.3 pF, n = 24). Cells with series resistance (obtained as $\tau_{VC/Cm}$) changes greater than 15% were discarded. EPSCs were evoked by mossy fiber stimulation at 0.05 Hz using comparable stimulus intensities in both genotypes (WT, 7 ± 0.6 V, n = 13, and NR2C-2B mice, 9 ± 0.9 V, n = 24) and were completely blocked by AP5 (30 μM) in both genotypes (data not shown). CP-101,606 was kindly provided by Pfizer, Inc. (Croton, USA). Data are expressed as mean ± SEM, and P values represent the results of independent two-tailed t tests.

Organotypic slice cultures of mouse cerebellum

Sagittal cerebellar slices (400 μm) from P8 wild-type or NR2C-2B mice were cut using a tissue cutter (McIllwain), transferred onto humidified membranes (Millicell-CM, Millipore), and cultured on a liquid layer of Neurobasal containing B27 supplement and glutamax I (2 mM, all Gibco BRL) in a humidified atmosphere with 5% CO_2 at 37°C for up to 12 days in vitro (DIV 12; Schrenk et al., 2002). Slice cultures were fixed after DIV 6 to DIV 12 with 4% PFA in 0.1 M phosphate buffer (PB). Calbindin D-28K (rabbit, 1:2000, SWant), NeuN (mouse, 1:1000, Chemicon), and TAG-1 (mouse clone 4D7, 1:3, DSHB) immunostaining was visualized with appropriate Cy2- and Cy3-labeled goat secondary antibodies (all at a dilution of 1:500). Quantitative analysis was performed from digital images obtained with a high resolution CCD camera. Results are expressed as means ± SEM, data were compared using unpaired t tests.

Histology

Three to six mice in each experimental group were transcardially perfused with 4% paraformaldehyde in PBS (pH = 7.4) under deep anesthesia with ketamine–xylazine (10–100 mg/kg). After overnight postfixation, 30 μm midsagittal sections were prepared by a cryostat (Leica), mounted on gelatinized glass slides, and Nissl stained. Sections from the vermal region were analyzed with the LUCIA software, using a Nikon Eclipse E600 microscope and a DVC 1300C camera. The thickness of the external granule layer, molecular layer, or internal granule layer in the same region of lobules 3, 4/5, and 8 was determined in four to six midsagittal sections from each animal. The mean values per lobuli were averaged within genotypes. The differences between NR2C-2B and control animals were investigated using the Mann–Whitney U test ($P < 0.05$).

Granule cell density and the average diameter of granule cells in the IGL were determined in the vermal regions of lobule 4/5 of 3 WT and 2 NR2C-2B mice. Six Nissl-stained slices were investigated from each animal using the NeuroLucida software on an Olympus BX51 microscope. To assess granule cell density, cells were counted in five 20.5 × 20.5 μm counting frames, positioned 100 μm apart in the middle of the IGL. Using an unbiased counting method, all the cells that came into focus inside the frame were counted and cell number was correlated to the apparent thickness of the counting frame. Average granule cell diameter was determined by measuring the maximum diameter of 75 randomly chosen granule cells in the IGL in each wild-type and NR2C-2B animal. Data were compared using Student's t test ($P < 0.05$).

Ultrastructural analyses

Three-month-old littermates (three wild-type and three mutant animals) were deeply anesthetized and transcardially perfused with 3.5% paraformaldehyde, 0.5% glutaraldehyde, and 1% picric acid in 0.1 M phosphate buffer (PB). Brains were postfixed without glutaraldehyde for additional 2 days at 4°C. Sixty-micrometer-thick sagittal Vibratome sections were cut from the cerebellar vermis. Four to five tissue slices of each cerebellum were osmicated (1% OsO_4 in PB for 1 h), dehydrated, and embedded

in Durcupan ACM (Fluka, Buchs, Switzerland). Cerebellar lobule 10 were cut and glued on the surface of blank Durcupan blocks. Sixty-nanometer ultra thin sections were cut by a Leica Ultramicrotome, collected on Formvar-coated single shot grids, and after further lead contrasting (0.2% lead citrate) analyzed under a JEOL JEM 100B electron microscope. Serial electron microscopic pictures were taken throughout the molecular layer, perpendicular to the pial surface. At least two sections were analyzed from each animal at a magnification of ×11900. In total, 128 wild-type and 103 NR2B/2C-pictures were taken in six and eight series of pictures, respectively. Pictures were developed onto photopaper with final ×25300 magnification. Excitatory synapses were counted on each picture based on the criteria that both presynaptic vesicles and postsynatic density in the dendritic spines should be clearly visible. Both wild-type and NR2C-2B data were fitted well with a normal distribution ($P < 0.0004$ and $P < 0.05$, respectively). Distributions were analyzed by one-way ANOVA.

Motor coordination learning

Male NR2C-2B mice ($n = 10$) and wild-type littermates ($n = 9$) were examined at different ages. The acclimatization period to the housing conditions during the experiment was 1 week and the animals were weighed daily and habituated to handling in the course of this week. The animals were maintained on a 12:12-h light/dark cycle and were tested during the light phase. Motor coordination and plasticity were tested using a custom-made fixed speed (12 rpm, 20 mm diameter) or a commercially available accelerating rotarod (TSE, Germany). The originally described experimental design of Jones and Roberts, 1968 was modified in a way that mice were subjected to three daily trials (intertrial interval 1 min) for three consecutive days. In the accelerating rotarod tests, mice were placed on the rod, which thereafter was accelerated to a speed up to 40 rpm over a period of 5 min. The time until the animal fell off the rod was registered with a cutoff after 5 min. In case of the fixed speed rotarod, animals were placed on the revolving rod for 2 min and the number of fallings together with the average time spent on the rod was recorded. For the analysis of behavior, two-tailed *t* tests for dependent and independent measures were used.

Acknowledgments

We thank Bernd Kirchherr and Christian Bayertz for excellent technical support, Prof. Rethelyi and Prof. Hamori for the access to the LUCIA and NeuroLucida image analyzer software, Prof. Seeburg and Dr. Sprengel for providing NR2C knock-out mice, and Dr. Takacs for providing electron microscopic facilities. This work was supported by the Deutsche Forschungsgemeinschaft (EI 243/2-2; SFB495, SFB505), by the German-Hungarian Academic Exchange Service (DAAD-MÖB), by the FKFP 0154/2001, OTKA F037769 grant (Hungarian Ministry of Education), and by the Förderprogramm Neurobiologie Baden-Württemberg.

References

Adcock, K.H., Metzger, F., Kapfhammer, J.P., 2004. Purkinje cell dendritic tree development in the absence of excitatory neurotransmission and of brain-derived neurotrophic factor in organotypic slice cultures. Neuroscience 127, 137–145.

Akazawa, C., Shigemoto, R., Bessho, Y., Nakanishi, S., Mizuno, N., 1994. Differential expression of five *N*-methyl-D-aspartate receptor subunit mRNAs in the cerebellum of developing and adult rats. J. Comp. Neurol. 347, 150–160.

Bessho, Y., Nawa, H., Nakanishi, S., 1994. Selective up-regulation of an NMDA receptor subunit mRNA in cultured cerebellar granule cells by K^+-induced depolarization an NMDA treatment. Neuron 12, 87–95.

Brandoli, C., Sanna, A., De Bernardi, M.A., Follesa, P., Brooker, G., Mocchetti, I., 2002. Brain-derived neurotrophic factor and bFGF down-regulate NMDA receptor function in cerebellar granule cells. J. Neurosci. 18, 7953–7961.

Contestabile, A., 2000. Roles of NMDA receptor activity and nitric oxide production in brain development. Brain Res. Rev. 32, 476–509.

Cull-Candy, S., Brickley, S., Farrant, M., 2001. NMDA receptor subunits: diversity, development and disease. Curr. Opin. Neurobiol. 11, 327–335.

D'Angelo, E., De Fillipi, G., Rossi, P., Taglietti, V., 1995. Synaptic excitation of individual rat cerebellar granule cells in situ: evidence for the role of NMDA receptors. J. Physiol. 484, 397–413.

Das, S., Sasaki, Y.F., Rothe, T., Premkumar, L.S., Takasu, M., Crandall, J.E., Dikkes, P., Conner, D.A., Rayudu, P.V., Cheung, W., Chen, H.S., Lipton, S.A., Nakanishi, N., 1998. Increased NMDA current and spine density in mice lacking the NMDA receptor subunit NR3A. Nature 393, 377–381.

Dingledine, R., Borges, K., Bowie, D., Traynelis, S.F., 1999. The glutamate receptor ion channels. Pharmacol. Rev. 51, 7–61.

Ebralidze, A.K., Rossi, D.J., Tonegawa, S., Slater, N.T., 1996. Modification of NMDA receptor channels and synaptic transmission by targeted disruption of the NR2C gene. J. Neurosci. 16, 5014–5025.

Farrant, M., Feldmeyer, D., Takahashi, T., Cull-Candy, S.G., 1994. NMDA-receptor channel diversity in the developing cerebellum. Nature 368, 335–339.

Furley, A.J., Morton, S.B., Manalo, D., Karagogeos, D., Dodd, J., Jessell, T.M., 1990. The axonal glycoprotein TAG-1 is an immunoglobulin superfamily member with neurite outgrowth-promoting activity. Cell 61, 157–170.

Hansel, C., Linden, D.J., D'Angelo, E.D., 2001. Beyond parallel fiber LTD: the diversity of synaptic and non-synaptic plasticity in the cerebellum. Nat. Neurosci. 4, 467–475.

Hatten, M.E., 1999. Central nervous system neuronal migration. Annu. Rev. Neurosci. 22, 511–539.

Hirai, H., Launey, T., 2000. The regulatory connection between the activity of granule cell NMDA receptors and dendritic differentiation of cerebellar Purkinje cells. J. Neurosci. 20, 5217–5224.

Hollmann, M., Heinemann, S., 1994. Cloned glutamate receptors. Annu. Rev. Neurosci. 17, 31–108.

Ito, M., 1984. Purkinje cells: morphology and development. The Cerebellum and Neural Control. Raven Press, New York, pp. 21–39.

Jones, B.J., Roberts, D.J., 1968. The quantiative measurement of motor inco-ordination in naive mice using an accelerating rotarod. J. Pharm. Pharmacol. 20, 302–304.

Kadotani, H., Hirano, T., Masugi, M., Nakamura, K., Nakao, K., Katsuki, M., Nakanishi, S., 1996. Motor discoordination results from combined gene disruption of the NMDA receptor NR2A and NR2C subunits, but not from single disruption of the NR2A or NR2C subunit. J. Neurosci. 16, 7859–7867.

Klein, M., Pieri, I., Uhlbach, F., Bayertz, C., van der Ploeg, A., Pfizenmaier, K., Eisel, U., 1998. Cloning of the promoter region of the murine NMDA receptor subunit $\varepsilon 2$: evidence for alternative splicing of the 5′ non coding region. Gene 208, 259–269.

Komuro, H., Rakic, P., 1993. Modulation of neuronal migration by NMDA receptors. Science 260, 95–97.

Komuro, H., Rakic, P., 1995. Dynamics of granule cell migration: a confocal microscopic study in acute cerebellar slice preparations. J. Neurosci. 15, 1110–1120.

Komuro, H., Yacubova, E., Rakic, P., 2001. Mode and tempo of tangential cell migration in the cerebellar external granular layer. J. Neurosci. 21, 527–540.

Kunimoto, M., Suzuki, T., 1997. Migration of granule neurons in cerebellar organotypic cultures is impaired by methylmercury. Neurosci. Lett. 226, 183–186.

Kutsuwada, T., Sakimura, K., Manabe, T., Takayama, C., Katakura, N., Kushiya, E., Natsume, R., Watanabe, M., Inoue, Y., Yagi, T., Aizawa, S., Arakawa, M., Takahashi, T., Nakamura, Y., Mori, H., Mishina, M., 1996. Impairment of suckling response, trigeminal neuronal pattern formation, and hippocampal LTD in NMDA receptor ε2 subunit mutant mice. Neuron 16, 333–344.

Laurie, D.J., Bartke, I., Schoepfer, R., Naujoks, K., Seeburg, P.H., 1997. Regional, developmental and interspecies expression of the four NMDAR2 subunits, examined using monoclonal antibodies. Brain Res., Mol. Brain Res. 51, 23–32.

Liesi, P., Stewart, R.R., Akinshola, B.E., Wright, J.M., 1999. Weaver cerebellar granule neurons show altered expression of NMDA receptor subunits both in vivo and in vitro. J. Neurobiol. 38, 441–454.

Luk, C.K., Kennedy, T.E., Sadikot, A.F., 2003. Glutamate promotes proliferation of striatal neuronal progenitors by an NMDA receptor-mediated mechanisms. J. Neurosci. 23, 2239–2250.

Marshall, J., Dolan, B.M., Garcia, E.P., Sathe, S., Tang, X., Mao, Z., Blair, L.A.C., 2003. Calcium channel and NMDA receptor activities differentially regulate nuclear C/EBPbeta levels to control neuronal survival. Neuron 39, 625–639.

Matsuda, K., Fletcher, M., Kamiya, Y., Yuzaki, M., 2003. Specific assembly with the NMDA receptor 3B subunit controls surface expression and calcium permeability of NMDA receptors. J. Neurosci. 23, 10064–10073.

Metzger, F., Kapfhammer, J.P., 2003. Protein kinase C: its role for Purkinje cell dendritic development and plasticity. Cerebellum 2, 206–214.

Monyer, H., Burnashev, N., Laurie, D.J., Sakmann, B., Seeburg, P.H., 1994. Developmental and regional expression in the rat brain and functional properties of four NMDA receptors. Neuron 12, 529–540.

Mori, H., Manabe, T., Watanabe, M., Satoh, Y., Suzuki, N., Toki, S., Nakamura, K., Yagi, T., Kushiya, E., Takahashi, T., Inoue, Y., Sakimura, K., Mishina, M., 1998. Role of the carboxy-terminal region of the GluRε2 subunit in synaptic localization of the NMDA receptor channel. Neuron 21, 571–580.

Nabekura, J., Ueno, T., Katsurabayashi, S., Furuta, A., Akaike, N., Okada, M., 2002. Reduced NR2A expression and prolonged decay of NMDA receptor-mediated synaptic current in rat vagal motoneurons following axotomy. J. Physiol. 539.3, 735–741.

Palay, S.L., Chan-Palay, V., 1974. Cerebellar Cortex: Cytology and Organization. Springer Press, New York, pp. 348.

Pieri, I., Klein, M., Bayertz, C., Gerspach, J., van der Ploeg, A., Pfizenmaier, K., Eisel, U., 1999. Regulation of the murine NMDA-receptor-subunit NR2C promoter by Sp1 and fushi tarazu factor1 (FTZ-F1) homologues. Eur. J. Neurosci. 11, 2083–2092.

Rossi, D.J., Slater, N.T., 1993. The developmental onset of NMDA receptor-channel activity during neuronal migration. Neuropharmacology 32, 1239–1248.

Rossi, P., Sola, E., Taglietti, V., Borchardt, T., Steigerwald, F., Utvik, J.K., Ottersen, O.P., Koehr, G., D'Angelo, E., 2002. NMDA receptor 2 (NR2) C-terminal control of NR open probability regulates synaptic transmission and plasticity at a cerebellar synapse. J. Neurosci. 22, 9687–9697.

Rumbaugh, G., Vicini, S., 1999. Distinct synaptic and extrasynaptic NMDA receptors in developing cerebellar granule neurons. J. Neurosci. 19, 10603–10610.

Schrenk, K., Kapfhammer, J.P., Metzger, F., 2002. Altered dendritic development of cerebellar Purkinje cells in slice cultures from protein kinase Cgamma-deficient mice. Neuroscience 110, 675–689.

Seil, F.J., 1996. Neural plasticity in cerebellar cultures. Prog. Neurobiol. 50, 533–556.

Sprengel, R., Suchanek, B., Amico, C., Brusa, R., Burnashev, N., Rozov, A., Hvalby, O., Jensen, V., Paulsen, O., Andersen, P., Kim, J.J., Thompson, R.F., Sun, W., Webster, L.C., Grant, S.G., Eilers, J., Konnerth, A., Li, J., McNamara, J.O., Seeburg, P.H., 1998. Importance of the intracellular domain of NR2 subunits for NMDA receptor function in vivo. Cell 92, 279–289.

Stuart, G.J., Dodt, H.U., Sakmann, B., 1993. Patch-clamp recordings from the soma and dendrites of neurons in brain slices using infrared video microscopy. Pflüegers Arch. 423, 511–518.

Solecki, D.J., Liu, X.L., Tomoda, T., Fang, Y., Hatten, M.E., 2001. Activated Notch2 signaling inhibits differentiation of cerebellar granule neuron precursors by maintaining proliferation. Neuron 31, 557–568.

Takács, J., Hámori, J., 1994. Developmental dynamics of Purkinje cells and dendritic spines in rat cerebellar cortex. J. Neurosci. Res. 38, 515–530.

Takács, J., Gombos, G., Görcs, T., Becker, T., de Barry, J., Hámori, J., 1997. Distribution of metabotropic glutamate receptor type 1a in Purkinje cell dendritic spines is independent of the presence of presynaptic parallel fibers. J. Neurosci. Res. 50, 433–442.

Takahashi, T., Feldmeyer, D., Suzuki, N., Onodera, K., Cull-Candy, S.G., Sakimura, K., Mishina, M., 1996. Functional correlation of NMDA receptor ε subunits expression with the properties of single-cahnnel and synaptic currents in the developing cerebellum. J. Neurosci. 16, 4376–4382.

Tanaka, M., Tomita, A., Yoshida, S., Yano, M., Shimizu, H., 1994. Observation of the highly organized development of granule cells in rat cerebellar organotypic cultures. Brain Res. 641, 319–327.

Watanabe, M., Mishina, M., Inoue, Y., 1994. Distinct spatiotemporal expressions of five NMDA receptor channel subunit mRNAs in the cerebellum. J. Comp. Neurol. 343, 513–519.

Watanabe, D., Inokawa, H., Hashimoto, K., Suzuki, N., Kano, M., Shigemoto, R., Hirano, T., Toyama, K., Kaneko, S., Yokoi, M., Moriyoshi, K., Suzuki, M., Kobayashi, K., Nagatsu, T., Kreitman, R.J., Pastan, I., Nakanishi, S., 1998. Ablation of cerebellar Golgi cells disrupts synaptic integration involving GABA inhibition and NMDA receptor activation in motor coordination. Cell 95, 17–27.